

PAPER

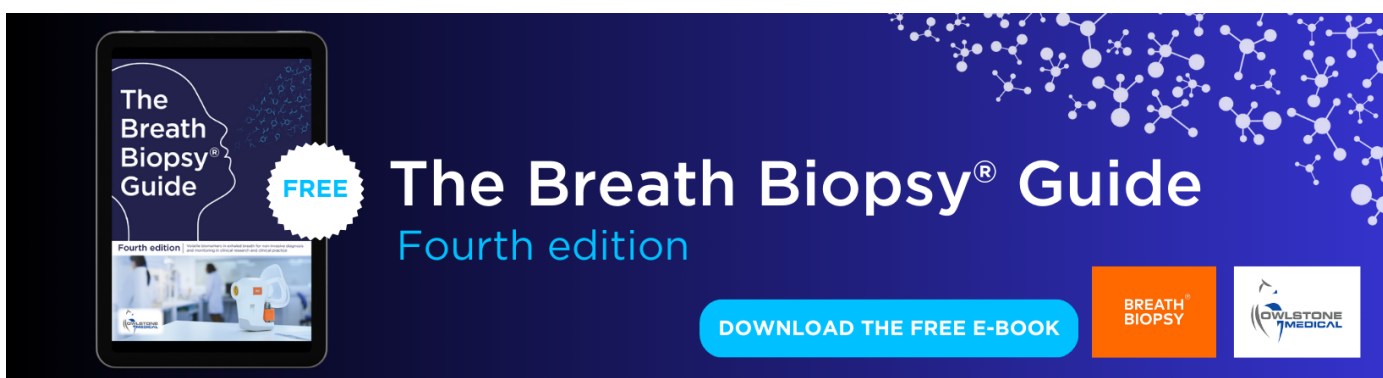
Multiscale network representation of physiological time series for early prediction of sepsis

To cite this article: Supreeth P Shashikumar *et al* 2017 *Physiol. Meas.* **38** 2235

View the [article online](#) for updates and enhancements.

You may also like

- [Advanced analyses of physiological signals in the neonatal intensive care unit](#)
J Huvanandana, C Thamrin, M B Tracy et al.
- [Increased sample asymmetry and memory of cardiac time-series following endotoxin administration in cirrhotic rats](#)
Mina Taghipour, Golnar Eftekhari, Zahra Haddadian et al.
- [Simultaneous Quantitative Detection of IL-6 and PCT Using SERS magnetic immunoassay with sandwich structure](#)
Xiaomei Wang, Li Ma, Cunming Hu et al.



The Breath Biopsy® Guide
Fourth edition

FREE

DOWNLOAD THE FREE E-BOOK

BREATH BIOPSY

OWLSTONE MEDICAL

Multiscale network representation of physiological time series for early prediction of sepsis

Supreeth P Shashikumar¹ , Qiao Li³, Gari D Clifford^{2,3} and Shamim Nemati^{3,4}

¹ Department of Electrical and Computer Engineering, Georgia Institute of Technology, Atlanta, GA, United States of America

² Department of Biomedical Engineering, Georgia Institute of Technology, Atlanta, GA, United States of America

³ Department of Biomedical Informatics, Emory University School of Medicine, Atlanta, GA, United States of America

E-mail: shamim.nemati@alum.mit.edu

Received 28 July 2017, revised 23 October 2017

Accepted for publication 1 November 2017

Published 29 November 2017



CrossMark

Abstract

Objective and Approach: Sepsis, a dysregulated immune-mediated host response to infection, is the leading cause of morbidity and mortality in critically ill patients. Indices of heart rate variability and complexity (such as entropy) have been proposed as surrogate markers of neuro-immune system dysregulation with diseases such as sepsis. However, these indices only provide an average, one dimensional description of complex neuro-physiological interactions. We propose a novel multiscale network construction and analysis method for multivariate physiological time series, and demonstrate its utility for early prediction of sepsis. **Main results:** We show that features derived from a multiscale heart rate and blood pressure time series network provide approximately 20% improvement in the area under the receiver operating characteristic (AUROC) for four-hour advance prediction of sepsis over traditional indices of heart rate entropy (0.78 versus 0.66). Our results indicate that this improvement is attributable to both the improved network construction method proposed here, as well as the information embedded in the higher order interaction of heart rate and blood pressure time series dynamics. Our final model, which included the most commonly available clinical measurements in patients' electronic medical records and multiscale entropy features, as well as the proposed network-based features, achieved an AUROC of 0.80. **Significance:** Prediction of the onset of sepsis prior to clinical recognition will allow for meaningful earlier interventions

⁴ Author to whom any correspondence should be addressed.

(e.g. antibiotic and fluid administration), which have the potential to decrease sepsis-related morbidity, mortality and healthcare costs.

Keywords: sepsis, multiscale network, blood pressure, predictive analytics, network physiology, intensive care, critical care

(Some figures may appear in colour only in the online journal)

1. Introduction

Sepsis is a significant healthcare burden with high morbidity and mortality among intensive care unit (ICU) patients. Prompt recognition and treatment are central to optimizing outcomes, yet antecedent signs and symptoms of sepsis can be subtle and unrecognized by clinicians despite continuous patient monitoring.

In recent years, machine-learning-based predictive algorithms for early prediction of septic shock have been proposed (Henry *et al* 2015, Ghosh *et al* 2017) with AUROC values in the range of 0.80–0.85. However, hemodynamic management through fluid and vasopressor administration are the only available intervention in septic patients at risk for shock, with a recent study suggesting that such interventions may not be associated with lower in-hospital mortality (Seymour *et al* 2017).

Using a machine-learning-based algorithm to predict sepsis with enough lead-time could prevent its occurrence in those deemed high risk if antibiotics are initiated before sepsis onset. Desautels and colleagues used a proprietary machine learning algorithm with commonly available clinical measurements in an electronic medical record (EMR) to predict sepsis four hours before it occurred (Desautels *et al* 2016); however, prediction of sepsis has proved to be difficult (AUROC 0.74). This may be partially due to the fact that early prediction of sepsis requires up-to-date clinical measurements, which are more likely to be available if there is already a clinical suspicion of infection (as in the case of septic shock prediction). Even when up-to-date clinical measurements are available, such data tends to have a low temporal resolution (once every 30 min or lower), and is subject to recall and information bias. For instance, blood pressure documentation by bedside clinicians can be biased towards normal when compared to corresponding blood pressure waveforms (Hug *et al* 2011), in part due to back-documentation of past data. However, incorporation of continuous high-resolution data (such as second-by-second vital signs time series from bedside monitors) has the potential to mitigate the aforementioned problems, and provide a more timely prediction of sepsis.

Sepsis is known as a dysregulated immune-mediated host response to infection. Alteration in heart rate (HR) and blood pressure (BP) variability and coupling prior to onset of sepsis has been reported in the literature (Buchman 2004, Moorman *et al* 2011) and potential links to neuro-immune system interactions have been established. According to the anti-inflammatory reflex model (Huston and Tracey 2011), pathogen-induced inflammation increases the activity of the vagus nerve, which controls the production of pro-inflammatory cytokines and prevents tissue damage. Although the relationship amongst inflammation, vagus nerve activity, heart rate variability (HRV), and baroreflex control of BP and HR is complex, this model suggests that monitoring indices of heart rate variability and complexity (as markers of vagus nerve activity) may provide useful surrogate markers of the inflammatory reflexes in health and disease.

Entropy is a measure of unpredictability of the state of a system, or equivalently of its average information content. Information can be thought of as a measure of surprise, and entropy can be thought of as a measure of average surprise. In recent years, one of the novel

advances in time series representation and quantification has been the mapping of time series to networks, based on ideas such as transition probabilities (Nicolis *et al* 2005, Campanharo *et al* 2011), visibility (Luque *et al* 2009, Lacasa *et al* 2015), and correlations (Steinhauser *et al* 2008, Yang and Yang 2008). Each of these studies demonstrated that many characteristics of time series can be extracted from the properties of the corresponding network. Moreover, network-based representations are capable of extracting more nuanced characteristics of time series.

In particular, the concept of modularity has been used to characterize time series (Sun and Deem 2007). By modularity, we mean a set of densely connected nodes within a network. Other authors have used the terms ‘cluster’ or ‘communities’ (Girvan and Newman 2002, Duch and Arenas 2005, Fortunato 2010) to denote such constellations of nodes. Networks with high modularity have dense connections between the nodes within modules, but sparse connections between nodes in different modules. An interpretation of what these modules represent is in terms of ‘set points’ of a system. Classical physiology is grounded on the principle of homeostasis, in which regulatory mechanisms act to maintain a steady state, i.e. ‘set point’. However, as argued by Ary Goldberger *et al* in his editorial (Goldberger 2001), many physiological systems tend to operate out of equilibrium and in locally stable regimes (several set points versus a single set point), hence the observation of modularity in the resulting networks of joint HR and BP time series.

Therefore, an aim of this study was to investigate the connection between HR and BP time series structures—as captured through quantification of the structure of their corresponding network representations—and early signs of sepsis. However, physiological time series can often exhibit complex patterns of variability over multiple timescales (Ivanov *et al* 1999, Costa *et al* 2002). For instance, time series of BP can exhibit oscillations on the order of seconds (e.g. due to the variations in sympathovagal balance), to minutes (e.g. as a consequence of fever, blood loss, or behavioral factors), to hours (e.g. due to humoral variations, sleep-wake cycle, or circadian effects) (Mancia 2012, Parati *et al* 2015). It should also be noted that interactions (or coupling) between physiological systems are often caused by distinct physiological mechanisms that operate across different timescales (Bartsch *et al* 2014). We therefore investigate the multiscale structure of vital signs networks, and their utility for early prediction of sepsis.

2. Materials and methods

This section describes the dataset used, as well as the proposed algorithm for prediction of sepsis, and the evaluation methods. All data processing, creation of networks, feature extraction, and classifier training and testing were performed using Matlab R2016b (MATLAB 2016).

2.1. Dataset

Heart rate (HR) and mean arterial blood pressure (MAP) time series at 2 s resolution were collected from bedside monitors in an Emory affiliated ICU, using the BedMaster system (Excel Medical Electronics, Jupiter FL, USA); a third-party software connected to the hospitals general electric (GE) monitors for the purpose of electronic data extraction and storage of high resolution waveforms. All adult ICU units were included in this study, including medical and surgical, cardiac care, and neuro-intensive care units. The bedside monitor data was then matched and time synchronized to each patient’s EMR data. A total of 100 patients (22%) met the definition of sepsis by Seymour *et al* (2016) at some point during their ICU stay. Specifically, all episodes of suspected infection ($t_{\text{suspicion}}$) were identified as the earlier

timestamp of antibiotics and blood cultures within a specific time span; if the antibiotic was given first, the culture sampling must have been obtained within 24 h. If the culture sampling was first, the antibiotic must have been ordered within 72 h. The onset time of sepsis (t_{sepsis}) was then defined as an episode of suspected infection with a two or more points change in the sequential organ failure assessment (SOFA) score from up to 48 h before to up to 24 h after the $t_{\text{suspicion}}$. The average length of hospital stay (LOS) among the septic patients was 137.6 [68.2–295.7] h, and the percentages of in-hospital mortality and in-patient hospice were 15.2% and 13.5%, respectively. The septic patients exhibited a higher average SOFA score compared to non-septic patients (4.8 [3.1–6.8] versus 1.6 [0.6–3.4]).

2.2. Model

Our goal is to define a set of physiological states that are represented by the nodes of a network. Transitions among these physiological states are captured by the network edges, and the network structure thereby captures the state trajectory through time.

Dynamic Bayesian networks have been used to model the trajectory of the state of physiological systems (Lehman *et al* 2015), where a system's *state* refers to a set of (observed or latent) attributes of the system that summarize all one needs to know about the system to predict its evolution through time (Buchman 1996). Parametric approaches such as the switching dynamical systems (Quinn *et al* 2009) assume the states transition dynamics to follow a Markov chain. The approach taken in this work is non-parametric, and extracts a set of system states via adaptive partitioning of the state-space. The partitions define the nodes in the corresponding network representation of the time series, and the transition probabilities are captured by the edges.

2.2.1. Defining the state-space. Time-lagged embedding provides information on the underlying dynamical system without having direct access to all the system variables (Takens *et al* 1981). As a first step to defining the state-space, we applied timed-lagged embedding (of order l) to each time series dimension. Next, the embedded time series samples were replaced by their rank orders (via rank order transformation) to achieve robustness to outliers. This step exploited the fact that mutual information between a set of random variables is invariant to invertible transformations such as the rank order transformation. Next, we partitioned the resulting state-space using an adaptive partitioning algorithm, as described next.

2.2.2. The Darbellay–Vajda (DV) partitioning algorithm. As shown in figure 1 the DV partitioning algorithm allows us to partition the state-space associated with a multivariate time series into varying size bins (or hypercubes), for the purpose of density estimation (Hudson 2006). Such DV partitioning was previously shown to be effective in calculating transfer entropy (Lee *et al* 2012, Nemati *et al* 2013), a statistical measure of the amount of directed entropy transfer between two random processes, and was shown to have lower computational cost than the competing methods. Similarly to the method of variable-bandwidth kernel density estimation (Terrell and Scott 1992), the DV partitioning algorithm automatically adjusts the bin (partition) size, depending on the density and local distribution of the data points, but requires no *a priori* assumption on the Kernel bandwidth, and is computationally more efficient to evaluate (Lee *et al* 2012). This is in contrast to the equipartitioning scheme (aka, a multidimensional histogram) where the entire state-space is split into equal partitions, which is an inefficient method for representing non-uniformly distributed data (see figure 2).

The DV partitioning algorithm involves recursively dividing the state-space into more refined partitions, based on the chi-squared test statistic (that checks whether the data in the

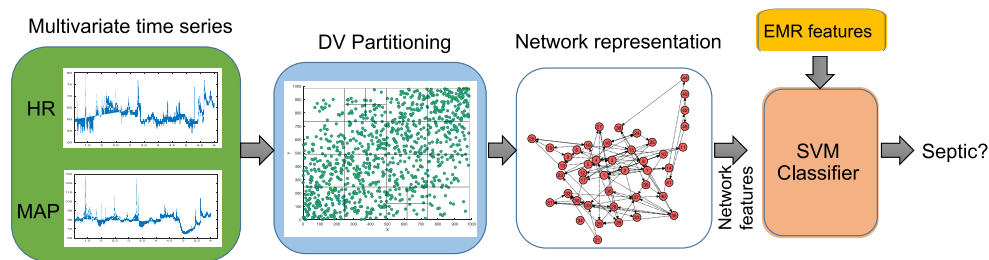


Figure 1. Schematic diagram of the proposed algorithm. The DV partitions obtained from the space of time-lagged HR and MAP time series are transformed to a network g —which consists of a set of nodes and an adjacency matrix. Every timescale will have a corresponding network. Various topological attributes and features derived from the constructed networks are used as inputs to the SVM classifier. In addition to the network attributes, EMR features are also fed into the SVM classifier.

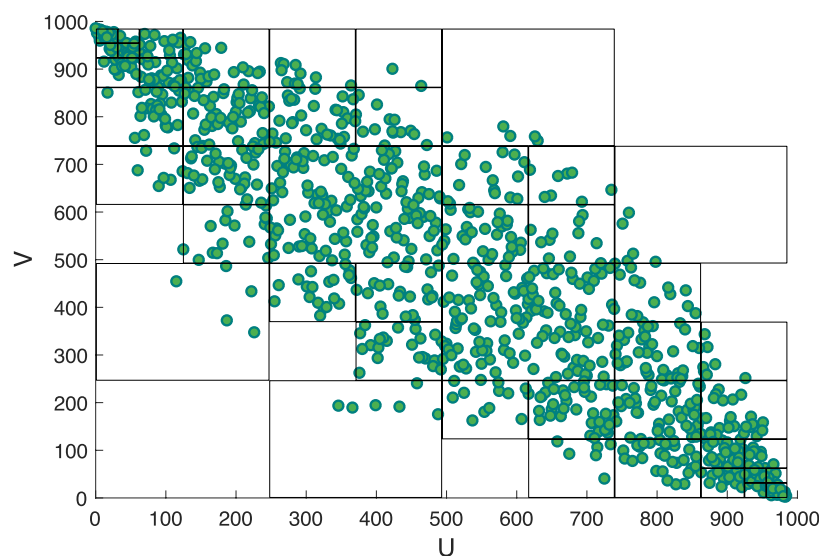


Figure 2. A two-dimensional visualization of DV partitioning. The observation space consists of 1000 data points sampled from a bivariate Gaussian distribution with $\sigma_{xy} = -0.9$, $\sigma_x^2 = 1$, and $\sigma_y^2 = 1$. The figure shows the observation space after ordinal sampling. It can be observed that densely populated regions in the space have smaller partitions, in comparison to fewer partitions created in sparser areas.

proposed partitioned cells are uniformly distributed). Let us consider a bivariate (two-dimensional) time series, $X = [x_1, x_2, \dots, x_T]$ and $Y = [y_1, y_2, \dots, y_T]$, where T is the length of the time series. First, a non-linear transformation is applied to X and Y , wherein the data in each time series are replaced by their rank orders (also called rank-order transformation). Let the rank order transformed time series be denoted by U and V respectively. We perform partitioning in the UV space as follows:

- (i) At every iteration, a bin (parent cell) is partitioned into smaller blocks (child cells), and we use the chi-squared test of independence to decide on the need for partitioning to child

cells or not. The null hypothesis for the chi-squared test is that the sample distribution in the parent cell is uniform.

- (ii) The chi-squared test statistic \mathcal{S} is given by

$$\mathcal{S} = \left(\sum_{i=1}^M \left(\frac{\sum N_i}{M} - N_i \right)^2 \right) / \sum_{i=1}^M \left(\frac{N_i}{M} \right) \quad (1)$$

where M is the total number of child cells for a parent cell, and N_i ($i = 1, \dots, N$) are the sample numbers.

- (iii) For a 5% significance level with three degrees of freedom, if \mathcal{S} is greater than $\chi^2_{95\%}(3)$, then the distribution of data is not uniform, and partitioning is continued. If not, the partitioning is stopped at that level. The level of statistical significance is a parameter that can be tuned.
- (iv) At first, the observation space is partitioned at the medians of U , V margins to generate four child cells. The Chi-squared test of independence is then performed; if the partitioning condition holds, the child cells are split into further smaller blocks (partitioned at the medians of their respective margins), and this continues recursively until the Chi-squared test statistic is no more satisfied across all cells.

The output of the partitioning algorithm is thus a list of partitions P , with each partition defined by a lower and upper bound in the observation space. An illustration of the DV partitioning algorithm for bivariate data is shown in figure 2 with the scatter plot of the data and the corresponding partitions obtained. It should be noted that the aforementioned procedure can be easily extended to any arbitrary N dimensional observation space.

2.2.3. Construction of network from partitions. Here we describe the process of construction of a network from a multivariate time series X . An example of a multivariate time series would be the HR and MAP time series recorded from a single subject. Given a list of partitions P , a map $M : T \Rightarrow G$ can be defined from the time domain T to the network domain G . More formally, let us define a map M from time domain $X \in T$ to a network $g \in G$, where $X = \{X_1, X_2, \dots, X_k\}$, k is the total number of time series recorded for each subject (in the above example, since HR and MAP are recorded for every subject, $k = 2$), and $X_i \in \mathbb{R}^L$, with L being the length of the time series, and $g = \{S, A\}$ consisting of a set of nodes S and adjacency matrix A . The total number of nodes N corresponds to the total number of partitions obtained from the DV partitioning algorithm. Therefore, each partition p_i ($i = 1, \dots, N$) is assigned to a node $n_i \in N$ in the graph g . Every multidimensional data point in X is assigned to one of the partitions. The adjacency matrix A is an $N \times N$ matrix, in which a_{ij} corresponds to the transition from node n_i to node n_j . Two nodes n_i and n_j are connected in the network with a weight a_{ij} , with a_{ij} representing the total number of transitions from node n_i to n_j . Each partition p_i can be thought of as a dynamical state in a physiological system, and the a_{ij} values of the adjacency matrix represent the probability of transition between the dynamical states of the system. In the above example, we would thus construct one network from the bivariate time series (HR and MAP time series) recorded from the subject.

2.2.4. Multiscale network representation. Interactions in biological systems manifest on multiple timescales (Bartsch *et al* 2014), and the interactions may change in different ways at these different timescales. It may, therefore, be important to capture the multiscale nature of such interactions, to help differentiate between healthy and unhealthy individuals. For a one dimensional time series $[x_1, x_2, \dots, x_N]$, a coarse grained time series $\{y^{(\tau)}\}$, corresponding to

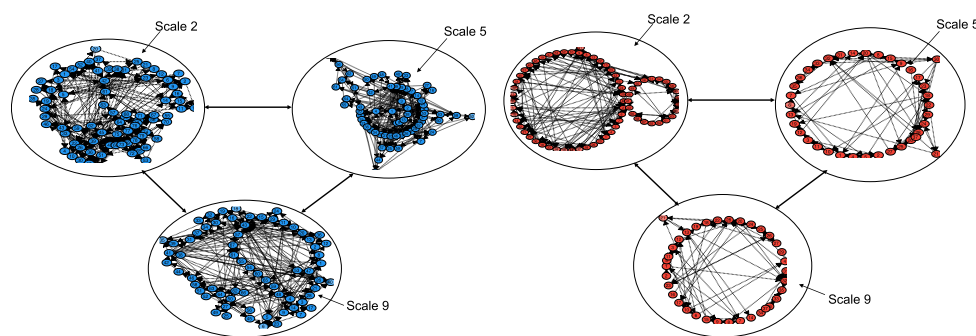


Figure 3. Examples of networks constructed from bivariate time series (HR and MAP) of a control (left panel) and a pre-septic (right panel) patient at different timescales. Within each of the networks, the arrows represent the transition from one node to another.

the scale factor τ was constructed as follows: first, the original time series was divided into non-overlapping windows of length τ ; second, the data points inside each window were averaged. In our experiments, we coarse-grained both HR and MAP according to the scale factor τ . Thus, for every scale factor τ_i ($i = 1, \dots, M$), where M is the total number of scale factors, a network G_i ($i = 1, \dots, M$) was constructed. Figure 3 provides a visualization of the networks constructed from bivariate time series (HR and MAP) of a control and a pre-septic patient at different timescales.

2.2.5. Network attributes for classification. In our proposed algorithm, for the network that we obtain as described in the previous sections, we compute many topological attributes, and use the derived features for classification. The following network attributes were computed for every network in the dataset: number of nodes (total number of nodes in the network), number of edges (total number of edges in the network), link density (total number of edges divided by the maximum possible edges in the network), average degree (average value of the degree of all nodes in the network, where the degree of a node is defined as the total number of its neighboring edges), number of loops (total number of independent loops in the network, also known as the ‘cyclomatic number’, or the number of edges that need to be removed so that the network contains no cycle), Loop3 (total number of loops of size 3 in the network), Loop4 (total number of loops of size 4 in the network), average clustering coefficient (clustering coefficient $c(u)$ for node u can be defined as the ratio of the number of actual edges between the neighbors of u to the number of possible edges between them, and the average clustering coefficient $C(G)$ of a network is the average of $c(u)$ taken over all the nodes in the network), Pearson coefficient (the Pearson correlation coefficient for a degree sequence, also known as the assortativity coefficient (Newman 2002)), algebraic connectivity (the second smallest Eigenvalue of the Laplacian matrix of a network, where the Laplacian matrix of a network is the difference between the sum of degrees of the diagonal elements in adjacency matrix and the adjacency matrix), closeness (average of $cc(u)$ taken over all the nodes in the network, where closeness centrality $cc(u)$ for node u is the inverse of sum of distance from node u to all other nodes in the network), average eccentricity (eccentricity of a node u is defined as $e(u) = \max\{d(u, v) : v \in V\}$, where the distance $d(u, v)$ is the length of the shortest path from u to v , and V is the set of all nodes. The average effective eccentricity is the average of effective eccentricities over all nodes in the network), maximum effective eccentricity (also known as the effective diameter; is defined as the maximum value of effective eccentricity over all nodes

in the graph), spectral radius (defined as the largest magnitude eigenvalue of the adjacency matrix of the network), trace (sum of the eigenvalues of the adjacency matrix, i.e. $\sum \lambda$), and energy (squared sum of the eigenvalues of the adjacency matrix A). More formally, the energy of a network G is $E(G) = \sum_i^n \lambda_i^2$.

2.2.6. Entropy and other EMR features. Socio-demographic features (age, gender, weight, race) were collected for every subject. We also included features that were commonly recorded by the bedside nurses, including mean arterial pressure (MAP), heart rate (HR), peripheral capillary oxygen saturation (SpO_2), systolic blood pressure (SBP), diastolic blood pressure (DBP), respiration rate (Resp), Glasgow coma score (GCS) and temperature (Temp). Each of the abovementioned features were quantized into eight levels, and each level was encoded into dummy binary representations. These discretized representations were then used in the classification model. We also extracted a few features that capture history, comorbidity and the clinical context of the patient, including Charlson comorbidity index, mechanical ventilation, unit information (surgical, cardiac care, or neuro-intensive care), as well as surgical speciality (cardiovascular, neuro, ortho-spine, oncology, urology, etc) and wound type (clean, contaminated, dirty or infected) if the patient had undergone surgery in the past 12 h.

We also calculated the following features from the HR and MAP time series (2 s resolution) derived from the bedside monitors proprietary software from the ECG and BP waveforms: standard deviation of HR (HR_{STD}), standard deviation of MAP (MAP_{STD}), multiscale entropy (Costa *et al* 2002) of (60/HR or RR intervals) and MAP (Over 17 Scales; RR_{MSE} , and MAP_{MSE} respectively)

2.3. Feature selection and classification

For every subject in the dataset, networks were constructed for timescales 1 through 10. A total of 16 network attributes were extracted from every constructed network. It is to be noted that the HR and MAP were each processed with a lag of order l . In addition to the network attributes, the Entropy and EMR features as described in section 2.2.6 were extracted. All the features were then used to train a support vector machine (SVM) classifier to predict onset of sepsis four hours ahead of time, based on the data from the preceding six hours. The output of the SVM was the probability of membership in the Sepsis class. Hyper-parameters of the model, including the timescale factors and lag order l were optimized using a Bayesian optimization technique (Ghassemi *et al* 2014).

For all continuous variables, we have reported the medians with inter-quartile range (IQR), and used a two-sided Wilcoxon ranksum test when comparing the septic and control populations. For binary features, we have reported the percentages, and used a two-sided Chi-squared test to assess differences in proportion between the septic and control populations. To assess the performance of the proposed algorithm on out-of-sample data, we performed a ten fold cross validation study. The features in the training set were transformed to have Gaussian distributions using either the identity, square root or logarithmic transformations. The transformation which provided the lowest k -statistic using the Lilliefors test was used on both training and test sets. The transformed data (both training and test data) was then normalized by subtracting the mean computed from the training set and dividing by the standard deviation computed from the training set. Feature transformation, training and classifier evaluation were performed separately for all ten folds. Area under the receiver operating characteristic (AUROC) curve, accuracy and specificity were calculated for training and test sets for all the folds. The sensitivity level was fixed at 0.85. We combined all the predictions (probability of being septic) across all the ten folds to report a single pooled AUROC (Airola *et al* 2009).

Table 1. Patient characteristics in the dataset.

	Control	Septic	<i>p</i> -value
<i>N</i>	100	150	—
Age	59.5 [46.0 68.0]	63.0 [47.5 72.5]	0.15
Male(%)	56%	48%	0.21
MAP	81.7 [75.0 90.1]	78.5 [70.3 91.3]	0.22
HR	84.8 [73.2 97.6]	92.5 [75.1 110.0]	<0.01
SpO ₂	97.6 [96.3 99.3]	97.9 [95.1 99.5]	0.32
SBP	126.0 [111.7 143.7]	121.2 [103.3 143.3]	0.20
DBP	60.0 [55.0 66.7]	58.3 [52.5 67.2]	0.25
Respiration rate	16.8 [14.2 18.7]	16.2 [2.25 20.4]	0.3
GCS	14.5 [10.0 15.0]	9.7 [6.0 14.3]	<0.01

3. Results

A total of 250 subjects were considered for this study. The median [IQR] age for the septic and control subjects was 63 [47.5 72.5] and 59.5 [46.0 68.0] respectively. The patient characteristics of the entire dataset have been tabulated in table 1. It can be observed that the onset of sepsis is associated with a drop in MAP as well as SBP, DBP, and a significant increase in HR (92.5 versus 84.8) and a significant decrease GCS (9.7 versus 14.5), reflecting a moderate loss of consciousness or alertness.

3.1. Construction of network based on HR and MAP

The most commonly selected scales and embedding dimension by the Bayesian optimization were scales 2, 3, 5, 6, 7, 9, and 10, lag order of 3. We therefore fixed these parameters across all experiments and model comparisons. We employed feature selection to find a minimum set of relevant features. The most commonly selected features across all scales included the average clustering coefficient, Pearson correlation coefficient, spectral radius, energy of graph, trace, and number of loops of size 4.

In the following experiments we used the graph attributes alone as features for the classifier. First, we constructed multiscale networks from HR alone, for which the pooled testing AUROC was 0.61. Next, we constructed multiscale networks from MAP alone, for which the pooled testing AUROC was 0.61. By combining HR and MAP, and constructing multiscale networks achieved a pooled testing AUROC of 0.78.

3.2. Classifier trained on combination of network, entropy and EMR features

Seven separate models were constructed, based on (1) multiscale entropy (MSE) features calculated from the HR and MAP time series, (2) EMR features including patient demographics, and other features described in section 2.2.6, (3) features extracted from multiscale network representation (MSNR), (4) combining the EMR features and entropy features (MSE + EMR), (5) combining MSNR and EMR features, (6) combining MSNR and MSE features, and (7) combining the EMR, MSNR and MSE features. The performance of the above models has been tabulated in table 2. The model based on MSNR features alone achieved a pooled testing AUROC of 0.78, with a corresponding sensitivity of 0.85 and specificity of 0.56. Combining the MSE features and MSNR features did not result in any improvement

Table 2. Performance summary of classifier trained on combinations of network, entropy and EMR features. Values shown are pooled AUROCs.

Model	Training AUROC	Testing AUROC
MSE	0.72	0.66
EMR	0.79	0.70
MSNR (MAP + HR)	0.85	0.78
MSE + EMR	0.83	0.73
MSNR + EMR	0.89	0.79
MSNR + MSE	0.85	0.75
MSNR + MSE + EMR	0.89	0.80

of AUROC (statistically insignificant). Combining EMR features and the MSNR features resulted in an improvement in AUC from 0.78 to 0.79 (statistically significant). For the model corresponding to MSNR + MSE + EMR features, the pooled AUROC on test set was 0.80 (statistically significant), with a specificity of 0.57 at 0.85 sensitivity level. The receiver operating characteristic (ROC) curves for the above models have been plotted in figure 4.

4. Discussion

We have shown that features derived from a multiscale HR and MAP time series network provide approximately 20% improvement over traditional indices of heart rate entropy in the AUROC for four-hour advance prediction of sepsis. This improvement is attributable to the information embedded in the higher order interaction of HR and MAP time series, as well as to the proposed novel approach to network construction, utilizing adaptive partitioning of the state-space to define a set of discrete states. This discretization method naturally trades off uncertainty in defining an event (a unique state) for a more accurate estimation of the probability of the event. The resulting algorithm is quick to implement, and readily extensible to multiscale analysis of the time series networks. Our final model, which includes the most commonly available clinical measurements in patients' electronic medical record (EMR) and multiscale entropy features, as well as the proposed network-based features, achieved an AUROC of 0.80 on the testing set.

The proposed network construction technique takes advantage of the fact that the mutual information between a set of random variables is invariant to invertible transformations such as the rank order transformation (replacing the data by their ranks). The rank order transformation makes the proposed technique robust to time series outlier samples with high amplitudes. Moreover, time-lagged embedding provides information on the underlying dynamical system without having direct access to all the system variables (Takens *et al* 1981). By applying the DV partitioning algorithm on the space of time-lagged embedded HR and MAP time series, we arrive at states that capture the non-linear dynamics of HR and MAP. Similarly to the method of variable-bandwidth kernel density estimation (Terrell and Scott 1992), the DV partitioning algorithm automatically adjusts the bin size (hypercubes), depending on the density and local distribution of the data points, but requires no *a priori* assumption on the kernel bandwidth, and is computationally more efficient to evaluate (Lee *et al* 2012).

Some of the most important features, including the average clustering coefficient, are reflective of the modularity of the network (networks with high modularity have dense connections between the nodes within modules but sparse connections between nodes in different modules). In graph theory, a clustering coefficient is a measure of the degree to which nodes

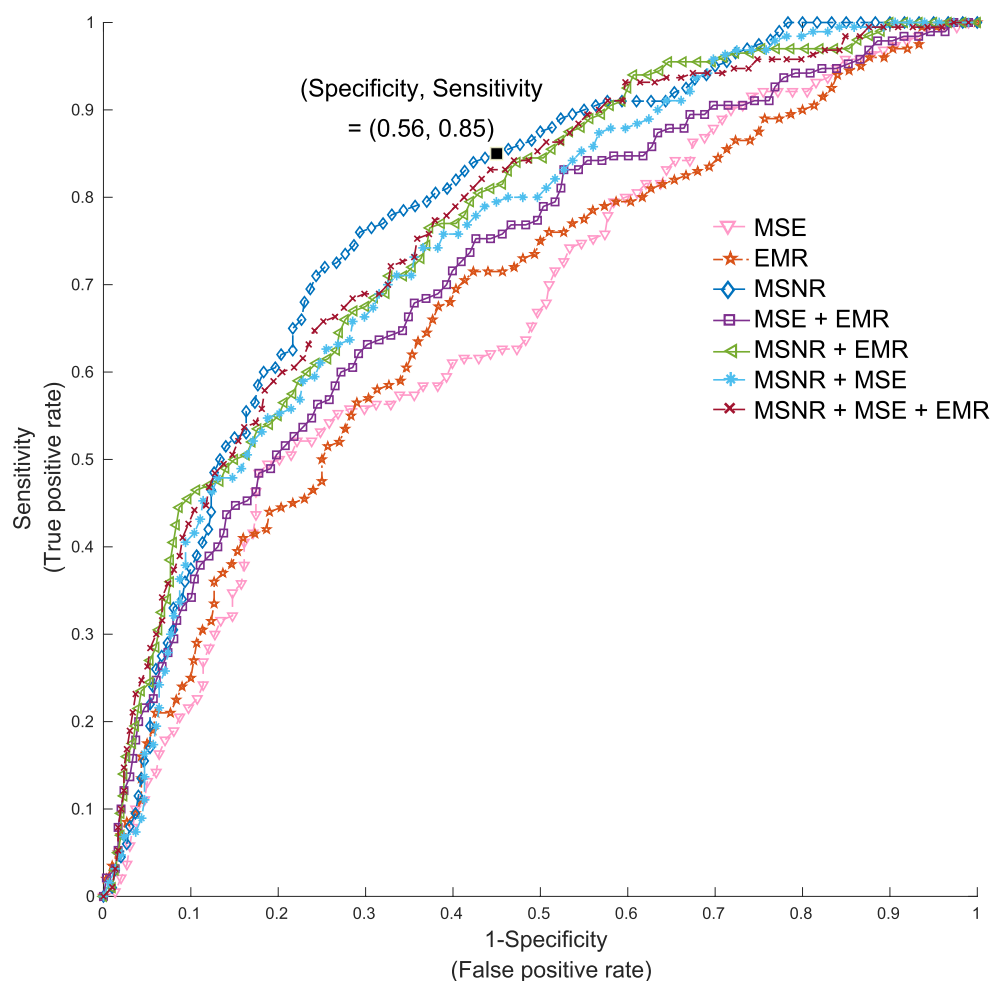


Figure 4. ROC curves for models based on combinations of network, entropy and EMR features. For the model corresponding to MSNR + MSE + EMR features, the AUROC on test set was 0.80, with a specificity of 0.57 at 0.85 sensitivity level. Notably, MSNR features alone achieved an AUC of 0.78, with the corresponding sensitivity (0.85) and specificity (0.56) marker on the plot.

in a graph tend to cluster together. Further study is needed to assess the correlation between the network features considered in this work and other commonly used predictive features within the literature. However, we hypothesize that the proposed framework provides a more generalizable set of features that are highly descriptive of the breakdown in autoregulatory mechanisms, and predictive of the eventual physiological decompensations, as in the case of sepsis. Notably, the multiscale nature of the proposed features provides robustness to the varying durations and timescales of physiological deterioration in critical care patients.

Many methods have been proposed in the literature to study human physiology as a complex network of interactions among body organs and processes. Much of the effort have been concentrated on identification and quantification of the interactions between these physiological processes (Ivanov and Bartsch 2014). Bashan *et al* (2012) proposed the concept of time delay stability (TDS) to quantify the dynamic interactions among physiological processes,

such as sleep and cardio-respiratory coupling. Building upon the concept of TDS, interactions across timescales and frequency bands have been explored to reveal dynamic interactions across body organs (Bartsch *et al* 2015, Liu *et al* 2015, Lin *et al* 2016). Utilizing the concept of ‘information dynamics’, entropy-based approaches have been proposed to quantify the information transfer between physiological processes (Lee *et al* 2012, Faes *et al* 2014). Our proposed MSNR approach complements other pioneering works in ‘Network Physiology’ by introducing a non-parametric approach to partitioning the state-space, and taking advantage of network analysis to quantify the non-linear interactions among multiple physiological time series.

Clinical decision support tools can help identify those at the highest risk for future sepsis. Although the existing works on utilization of EMR and laboratory data for prediction of sepsis seem promising (Lukaszewski *et al* 2008, Wang *et al* 2010, Desautels *et al* 2016), they are limited by low-frequency and often inconsistent data collected for purposes other than timely and accurate representation of patients’ physiology. Highly predictive features extracted directly from the high-resolution vital signs time series can improve sepsis prediction over low-resolution clinical data in ICU patients, and a high-performance prediction model can be derived from a combination of EMR and high-frequency physiologic data. A real-time system capable of early prediction of sepsis, followed by appropriate antibiotics therapy, will have a significant impact on the overall mortality and cost burden of this deadly disease (Seymour *et al* 2017).

Acknowledgments

SN is funded by the National Institutes of Health, award # K01ES025445. QL is partially funded by the Surgical Critical Care Initiative (SC2i), funded by the Department of Defense Defense Health Program Joint Program Committee 6 / Combat Casualty Care (USUHS HT9404-13-1-0032 and HU0001-15-2-0001). The opinions or assertions contained herein are the private ones of the author/speaker and are not to be construed as official or reflecting the views of the Department of Defense, the Uniformed Services University of the Health Sciences or any other agency of the US Government.

ORCID iDs

Supreeth P Shashikumar  <https://orcid.org/0000-0002-0348-4261>

References

- Airola A, Pahikkala T, Waegeman W, De Baets B and Salakoski T 2009 A comparison of AUC estimators in small-sample studies *Mach. Learn. Syst. Biol.* **8** 3–13
- Bartsch R P, Liu K K, Bashan A and Ivanov P C 2015 Network physiology: how organ systems dynamically interact *PLoS One* **10** e0142143
- Bartsch R P, Liu K K, Ma Q D and Ivanov P C 2014 Three independent forms of cardio-respiratory coupling: transitions across sleep stages *Computing in Cardiology Conf.* (IEEE) pp 781–4
- Bashan A, Bartsch R P, Kantelhardt J W, Havlin S and Ivanov P C 2012 Network physiology reveals relations between network topology and physiological function *Nat. Commun.* **3** 702
- Buchman T G 1996 Physiologic stability and physiologic state *J. Trauma Acute Care Surg.* **41** 599–605
- Buchman T G 2004 Nonlinear dynamics, complex systems, and the pathobiology of critical illness *Curr. Opin. Crit. Care* **10** 378–82

- Campanharo A S, Sirer M I, Malmgren R D, Ramos F M and Amaral L A N 2011 Duality between time series and networks *PloS One* **6** e23378
- Costa M, Goldberger A L and Peng C K 2002 Multiscale entropy analysis of complex physiologic time series *Phys. Rev. Lett.* **89** 068102
- Desautels T *et al* 2016 Prediction of sepsis in the intensive care unit with minimal electronic health record data: a machine learning approach *J. Med. Internet Res. Med. Inf.* **4** E28
- Duch J and Arenas A 2005 Community detection in complex networks using extremal optimization *Phys. Rev. E* **72** 027104
- Faes L, Nollo G, Jurysta F and Marinazzo D 2014 Information dynamics of brain–heart physiological networks during sleep *New J. Phys.* **16** 105005
- Fortunato S 2010 Community detection in graphs *Phys. Rep.* **486** 75–174
- Ghassemi M, Lehman L W, Snoek J and Nemati S 2014 Global optimization approaches for parameter tuning in biomedical signal processing: a focus on multi-scale entropy *Computing in Cardiology Conf. (IEEE)* pp 993–6
- Ghosh S, Li J, Cao L and Ramamohanarao K 2017 Septic shock prediction for ICU patients via coupled hmm walking on sequential contrast patterns *J. Biomed. Inf.* **66** 19–31
- Girvan M and Newman M E 2002 Community structure in social and biological networks *Proc. Natl Acad. Sci.* **99** 7821–6
- Goldberger A L 2001 Heartbeats, hormones, and health: is variability the spice of life? *Am. J. Respiratory Crit. Care Med.* **163** 1289–90
- Henry K E, Hager D N, Pronovost P J and Saria S 2015 A targeted real-time early warning score (trewscore) for septic shock *Sci. Trans. Med.* **7** 299ra122
- Hudson J E 2006 Signal processing using mutual information *IEEE Signal Process. Mag.* **23** 50–4
- Hug C W, Clifford G D and Reisner A T 2011 Clinician blood pressure documentation of stable intensive care patients: an intelligent archiving agent has a higher association with future hypotension *Crit. Care Med.* **39** 1006
- Huston J M and Tracey K J 2011 The pulse of inflammation: heart rate variability, the cholinergic anti-inflammatory pathway and implications for therapy *J. Intern. Med.* **269** 45–53
- Ivanov P C, Amaral L A N, Goldberger A L, Havlin S, Rosenblum M G, Struzik Z R and Stanley H E 1999 Multifractality in human heartbeat dynamics *Nature* **399** 461–5
- Ivanov P C and Bartsch R P 2014 *Networks of Networks: the Last Frontier of Complexity* (New York: Springer) pp 203–22
- Lacasa L, Nicosia V and Latora V 2015 Network structure of multivariate time series *Sci. Rep.* **5** 15508
- Lee J, Nemati S, Silva I, Edwards B A, Butler J P and Malhotra A 2012 Transfer entropy estimation and directional coupling change detection in biomedical time series *Biomed. Eng. Online* **11** 19
- Lehman L W H, Adams R P, Mayaud L, Moody G B, Malhotra A, Mark R G and Nemati S 2015 A physiological time series dynamics-based approach to patient monitoring and outcome prediction *IEEE J. Biomed. Health Inform.* **19** 1068–76
- Lin A, Liu K K, Bartsch R P and Ivanov P C 2016 Delay-correlation landscape reveals characteristic time delays of brain rhythms and heart interactions *Phil. Trans. R. Soc. A* **374** 20150182
- Liu K K, Bartsch R P, Lin A, Mantegna R N and Ivanov P C 2015 Plasticity of brain wave network interactions and evolution across physiologic states *Frontiers Neural Circuits* **9** 62
- Lukaszewski R A *et al* 2008 Presymptomatic prediction of sepsis in intensive care unit patients *Clin. Vaccine Immunol.* **15** 1089–94
- Luque B, Lacasa L, Ballesteros F and Luque J 2009 Horizontal visibility graphs: exact results for random time series *Phys. Rev. E* **80** 046103
- Mancia G 2012 Short-and long-term blood pressure variability *Hypertension* **60** 512–7
- MATLAB 2016 *Version 9.1 (R2016b)* (Natick, MA: The MathWorks Inc.)
- Moorman J R, Delos J B, Flower A A, Cao H, Kovatchev B P, Richman J S and Lake D E 2011 Cardiovascular oscillations at the bedside: early diagnosis of neonatal sepsis using heart rate characteristics monitoring *Physiol. Meas.* **32** 1821
- Nemati S, Edwards B A, Lee J, Pittman-Polletta B, Butler J P and Malhotra A 2013 Respiration and heart rate complexity: effects of age and gender assessed by band-limited transfer entropy *Respiratory Physiol. Neurobiol.* **189** 27–33
- Newman M E 2002 Assortative mixing in networks *Phys. Rev. Lett.* **89** 208701
- Nicolis G, Cantu A G and Nicolis C 2005 Dynamical aspects of interaction networks *Int. J. Bifurcation Chaos* **15** 3467–80

- Parati G, Ochoa J E, Lombardi C and Bilo G 2015 Blood pressure variability: assessment, predictive value, and potential as a therapeutic target *Curr. Hypertension Rep.* **17** 23
- Quinn J A, Williams C K and McIntosh N 2009 Factorial switching linear dynamical systems applied to physiological condition monitoring *IEEE Trans. Pattern Anal. Mach. Intell.* **31** 1537–51
- Seymour C W, Gesten F, Prescott H C, Friedrich M E, Iwashyna T J, Phillips G S, Lemeshow S, Osborn T, Terry K M and Levy M M 2017 Time to treatment and mortality during mandated emergency care for sepsis *New Engl. J. Med.* **376** 2235–44
- Seymour C W *et al* 2016 Assessment of clinical criteria for sepsis: for the Third International Consensus Definitions for Sepsis and Septic Shock (sepsis-3) *J. Am. Med. Assoc.* **315** 762–74
- Steinhauser D, Krall L, Müssig C, Büssis D and Usadel B 2008 Correlation networks *Analysis of Biological Networks* (New York: Wiley) ch 13, pp 305–33
- Sun J and Deem M W 2007 Spontaneous emergence of modularity in a model of evolving individuals *Phys. Rev. Lett.* **99** 228107
- Takens F *et al* 1981 Detecting strange attractors in turbulence *Lecture Notes Math.* **898** 366–81
- Terrell G R and Scott D W 1992 Variable kernel density estimation *Ann. Stat.* **20** 1236–65
- Wang S L, Wu F and Wang B H 2010 *Advances in Computational Biology* (New York: Springer) pp 75–81
- Yang Y and Yang H 2008 Complex network-based time series analysis *Physica A* **387** 1381–6